Anal. Chem. **2008,** *80,* 7075–7083

Label-Free DNA Sensor by Boron-Doped Diamond Electrode Using an ac Impedimetric Approach

Jian Weng,*,† Jianfeng Zhang,† Hui Li,† Liping Sun,*,† Chenghong Lin,† and Qiqing Zhang†,‡

Research Center of Biomedical Engineering, College of Materials, Technology Research Center of Biomedical Engineering of Xiamen City, The Key Laboratory of Biomedical Engineering of Fujian Province, Xiamen University, Xiamen 361005 (P. R. China), and Institute of Biomedical Engineering, Chinese Academy of Medical Science, Peking Union Medical College, The Key Laboratory of Biomedical Material of Tianjin, Tianjin 300192, P. R. China

An electrochemical biosensor using a boron-doped diamond (BDD) electrode is described for differentiating between gene sequences according to DNA hybridization events using an ac impedimetric approach. BDD electrodes were dipped into a 1% solution of polyethylenimine (PEI) to adsorb a thin layer of positively charged PEI on the surface of BDD, then PEI-modified BDD electrodes were used to immobilize negatively charged single-stranded PCR fragments from Exon 7 of human p53 gene. Alternating current impedimetric measurements were first performed on these systems in phosphate buffered saline (PBS) and then upon exposure to single-stranded DNA (ssDNA). When the ssDNA-immobilized BDD electrode and solution ssDNA were completely complementary, a large drop in impedance was measured. Complementary DNA could be clearly detected at concentrations down to 10^{-19} g mL^{-1} at a fixed frequency (10 Hz). Higher concentrations of DNA gave faster hybridization with saturation occurring at levels above 1.0 pg mL^{-1}. Responses were much lower upon exposure to noncDNA, even at higher concentrations. The results show it is possible to directly detect target DNA at a fixed frequency and without additional labeling.

Diamond type materials have become more widely available due to new gas or plasma deposition procedures and can be grown as single-, poly-, or nanocrystalline films, either by homo- or heteroepitaxy. Diamond as a high-performance material occupies a special place due to its extreme properties, e.g., hardness, chemical inertness, thermal conductivity, optical properties, and electric characteristics.[1−3] Work of our group and others over the past decade has shown that diamond also can be used as an electrode material with interesting applications in electroanalysis.[4−10] When made sufficiently electrically conducting, for example, by boron-doping, thin film boron-doped diamond (BDD) electrodes open up new opportunities for chemical and bioanalysis. Recently, BDD thin-film electrodes have been shown to possess interesting properties for electroanalysis over conventional types of electrode materials, including (i) a relatively low background current, (ii) a wide potential window in aqueous environments owing to the chemically inert surface suitable for corrosion-free oxidation process even under extreme conditions, and (iii) mechanical robustness for application.[11−25]

Diamond has recently become a promising candidate for bioelectronic devices as it shows good electronic and chemical properties and is considered to be biocompatible.[26−28] Depending

* To whom correspondence should be addressed. E-mail: jweng@xmu.edu.cn (J.W.); sunliping@xmu.edu.cn. (L.S.).

† Xiamen University.

‡ Peking Union Medical College.

(1) Rao, T. N.; Fujishima, A. *Diamond Relat. Mater.* **2000**, *9*, 383.
(2) Angus, J. C.; Martin, H. B.; Landau, U.; Evstefeeva, Y. E.; Miller, B.; Vinokur, N. *New Diamond Front. Carbon Technol.* **1999**, *9*, 175.
(3) Compton, R. G.; Foord, J. S.; Marken, F. *Electroanalysis* **2003**, *15*, 1349.
(4) Zhong, Y. L.; Chong, K. F.; May, P. W.; Chen, Z. K.; Loh, K. P. *Langmuir* **2007**, *23*, 5824.
(5) Sun, B.; Colavita, P. E.; Kim, H.; Lockett, M.; Marcus, M. S.; Smith, L. M.; Hamers, R. J. *Langmuir* **2006**, *22*, 9598.
(6) Shin, D.; Tokuda, N.; Rezek, B.; Nebel, C. E. *Electrochem. Commun.* **2006**, *8*, 844.
(7) Fortin, E.; Chane-Tune, J.; Delabouglise, D.; Bouvier, P.; Livache, T.; Mailley, P.; Marcus, B.; Mermoux, M.; Petit, J. P.; Szunerits, S.; Vieil, E. *Electroanalysis* **2005**, *17*, 517.
(8) Apilux, A.; Tabata, M.; Chailapakul, O. *Bioelectrochemistry* **2007**, *70*, 435.
(9) Krüger, A. *Angew. Chem., Int. Ed.* **2006**, *45*, 6426.
(10) Weng, J.; Xue, J.; Wang, J.; Ye, J. S.; Cui, H.; Shen, F. S.; Zhang, Q. *Adv. Funct. Mater.* **2005**, *15*, 639.
(11) Song, Y.; Swain, G. M. *Anal. Chem.* **2007**, *79*, 2412.
(12) Watanabe, T.; Ivandini, T. A.; Makide, Y.; Fujishima, A.; Einaga, Y. *Anal. Chem.* **2006**, *78*, 7857.
(13) Fortin, E.; Vieil, E.; Mailley, P.; Szunerits, S.; Livache, T. *Anal. Chem.* **2007**, *79*, 3741.
(14) O'Mullane, A. P.; Neufeld, A. K.; Harris, A. R.; Bond, A. M. *Langmuir* **2006**, *22*, 10499.
(15) Szunerits, S.; Mermoux, M.; Crisci, A.; Marcus, B.; Bouvier, P.; Delabouglise, D.; Petit, J. P.; Janel, S.; Boukherroub, R.; Tay, L. *J. Phys. Chem. B* **2006**, *110*, 23888.
(16) Ivandini, T. A.; Sato, R.; Makide, Y.; Fujishima, A.; Einaga, Y. *Anal. Chem.* **2006**, *78*, 6291.
(17) Bakker, E.; Qin, Y. *Anal. Chem.* **2006**, *78*, 3965.
(18) Rubio-Retama, J.; Hernando, J.; Lopez-Ruiz, B.; Hartl, A.; Steinmuller, D.; Stutzmann, M.; Lopez-Cabarcos, E.; Garrido, J. A. *Langmuir* **2006**, *22*, 5837.
(19) Ivandini, T. A.; Rao, T. N.; Fujishima, A.; Einaga, Y. *Anal. Chem.* **2006**, *78*, 3467.
(20) Tian, R. H.; Rao, T. N.; Einaga, Y.; Zhi, J. F. *Chem. Mater.* **2006**, *18*, 939.
(21) Batchelor-McAuley, C.; Banks, C. E.; Simm, A. O.; Jones, T. G. J.; Compton, R. G. *Analyst* **2006**, *131*, 106.
(22) Muna, G. W.; Quaiserova-Mocko, V.; Swain, G. M. *Anal. Chem.* **2005**, *77*, 6542.
(23) Stotter, J.; Show, Y.; Wang, S. H.; Swain, G. M. *Chem. Mater.* **2005**, *17*, 4880.
(24) Ji, X. B.; Banks, C. E.; Compton, R. G. *Analyst* **2005**, *130*, 1345.
(25) Hayashi, K.; Iwasaki, Y.; Horiuchi, T.; Sunagawa, K.; Tate, A. *Anal. Chem.* **2005**, *77*, 5236.
(26) Rezek, B.; Shin, D.; Nakamura, T.; Nebel, C. E. *J. Am. Chem. Soc.* **2006**, *128*, 3884.
(27) Fu, C.; Lee, H. Y.; Chen, K.; Lim, T. S.; Wu, H. Y.; Lin, P. K.; Wei, P. K.; Tsao, P. H.; Chang, H. C.; Fann, W. *Proc. Natl. Acad. Sci. U.S.A.* **2007**, *104*, 727.

10.1021/ac800610z CCC: $40.75
Published on Web 08/16/2008

on the chosen synthetic method, diamond materials exhibit significantly different surface properties. For example, hydrogenated diamond films have a highly hydrophobic character, which hinders the nonspecific adsorption of polar biomolecules.[29,30] In contrast, poly L-lysine, enzymes, or antibodies can be adsorbed on polar diamond surfaces. The presence of functional groups on the diamond surface also enables the covalent bonding of various moieties. Depending on the original surface coverage, different functionalization strategies, such as silanization, esterification, amidation, and direct C−C coupling have been applied. The aim of many of these investigations is the grafting of biologically active moieties, such as DNA, enzymes, or antibodies. The application of biofunctionalized diamond in, for example, bioassays or "lab on the chip" devices has been considered.[31] The covalent attachment of DNA molecules to modified diamond surfaces has been described by several groups. Takahashi and co-workers used terminal carboxyl groups to connect the DNA molecules through the formation of amide linkages.[32] Ando and co-workers described the grafting of DNA molecules through thymidines immobilized by ester bridges.[33] A much more stable coupling can be achieved by the formation of direct C−C bonds. In 2000, Takahashi et al. demonstrated the covalent attachment of DNA on polycrystalline diamond using a photochemical chlorination/amination/carboxylation of the initially H-terminated surface as initial steps.[34] In 2002, Yang et al. introduced an alternative method to modify nanocrystalline diamond surfaces with DNA.[35−37] The thin film of nanocrystalline diamond, even of submicrometer thickness, can be used as a highly stable substrate for selective biological modification and adsorption. Diamond is unique in its ability to achieve high selectivity and high stability, while it remains a challenge to improve the sensitivity for DNA detection in bioelectronic sensing systems.

Subsequent to molecular recognition at the surface, there has to be a method for detecting this event. Alternating current impedance measurement has been widely used to interrogate a variety of sensors. Some reports have shown the versatility of this technique for enzyme-based sensors.[38] The technique has also been applied to DNA detection; for example, hybridization can be followed by ac impedance techniques and can be used in this way to detect the presence of the Tay-Sachs mutant gene.[39] Hybridization to single-stranded DNA (ssDNA) with the complementary counterpart immobilized within polypyrrole, polyaniline, or polyethylenimine (PEI) has been detected by the use of ac impedance and allowed detection limits down to 1.0 fg mL^{-1} on different types of electrodes,[40,41] while hybridization with cDNA in solution could be detected by ac impedance studies or ellipsometry and allowed detection limits only down to 0.01 mg mL^{-1}.[42] Therefore the detection limit by ac impedance can be improved when the complementary counterpart of ssDNA is immobilized to a positively charged polymer surface. Many other methods are available to detect the hybridization of DNA: for example, fluorescent labeling-based microarrays are commonly used. This, combined with long reaction times (hours to days) and the need for expensive equipment, results in an overall high cost of these techniques. Eliminating the labeling steps is therefore required to produce "gene chips," providing a simple, accurate, stable, and inexpensive platform for patient diagnosis.[43] On the other hand, surface plasmon resonance (SPR), quartz crystal microbalance (QCM), and the mechanical cantilever array, which are label-free detection methods, achieve the high sensitivity and decrease the analytical process (without labeling), but these methods require highly precise and expensive instrumentation.

In an attempt to improve the sensitivity of DNA detection with BDD electrodes by ac impedance, we have used PCR-amplified DNA from the human p53 gene; the complementary counterpart of single-stranded DNA was immobilized to a positively charged polymer PEI on the BDD surface and ac impedance measurements were at a fixed frequency (10 Hz), rather than scanning across a range of frequencies. This technique can directly detect hybridization and offers many advantages in comparison to those that require labels.

EXPERIMENTAL SECTION

Polyethylenimine (PEI) (linear, $M_w = 25\,000$) was purchased from Alfa Aesar, and bovine serum albumin was from Aldrich. Disodium hydrogen orthophosphate, potassium dihydrogen orthophosphate, potassium chloride, and sodium chloride (analytical grade) were purchased from Green Bird Science and Technology Development (China). All chemicals were used without further purification. All solutions were prepared using Millipore (Model Milli-Q) purified water. The pH 7.4 buffer solution was made by dissolving KH_2PO_4 (0.24 g), Na_2HPO_4 (1.44 g), KCl (0.2 g), and NaCl (8.0 g) in water and making up to 1 L.

Point mutations at codon 248 (exon 7) and codon 273 (exon 8) are mutational "hotspots" of the p53 gene. All DNA oligonucleotides were purchased from Shanghai Sangon Biological Engineering Technology & Services Co., Ltd. The following sequences were synthesized:

7F: 5′-GCTCTGACTGTACCACCATCCA-3′
7R: 5′-ACCTGGAGTCTTCCAGTGTGA-3′

(28) Chong, K. F.; Loh, K. P.; Vedula, S. R. K.; Lim, C. T.; Sternschulte, H.; Steinmüller, D.; Sheu, F. S.; Zhong, Y. L. *Langmuir* **2007**, *23*, 5615.
(29) Delabouglise, D.; Marcus, B.; Mermoux, M.; Bouvier, P.; Chane-Tune, J.; Petit, J.-P.; Mailley, P.; Livache, T. *Chem. Commun.* **2003**, 2698.
(30) Clare, T. L.; Clare, B. H.; Nichols, B. M.; Abbott, N. L.; Hamers, R. J. *Langmuir* **2005**, *21*, 6344.
(31) Song, K.-S.; Kawarada, H. *New Diamond Front. Carbon Technol.* **2005**, *5*, 325.
(32) Takahashi, K.; Tanga, M.; Takai, O.; Okamura, H. *Diamond Relat. Mater.* **2003**, *12*, 572.
(33) Ushizawa, K.; Sato, Y.; Mitsumori, T.; Machinami, T.; Ueda, T.; Ando, T. *Chem. Phys. Lett.* **2002**, *351*, 105.
(34) Takahashi, K.; Tanga, M.; Takai, O.; Okamura, H.; Sakaki, Y. *Bio. Ind.* **2000**, *17*, 44.
(35) Yang, W.; Auciello, O.; Butler, J. E.; Cai, W.; Carlisle, J. A.; Gerbi, J. E.; Gruen, D. M.; Knickerbocker, T.; Lasseter, T. L.; Russell, J. N., Jr.; Smith, L. M.; Hamers, R. J. *Nat. Mater.* **2002**, *1*, 253.
(36) Strother, T.; Kickerbocker, T.; Russel, J. N., Jr.; Butler, J. E.; Smith, M. L.; Hamers, R. J. *Langmuir* **2002**, *18*, 968.
(37) Kickerbocker, T.; Strother, T.; Schwartz, M. P.; Russel, J. N., Jr.; Butler, J. E.; Smith, L. M.; Hamers, R. J. *Langmuir* **2003**, *19*, 1938.
(38) Grant, S.; Davis, F.; Law, K. A.; Higson, S. P. J.; Gibson, T. D. *Anal. Chim. Acta* **2005**, *537*, 163.
(39) Bardea, A.; Patolsky, F.; Dagan, A.; Willer, I. *Chem. Commun.* **1999**, 21.
(40) Davis, F.; Hughes, M. A.; Cossins, A. R.; Higson, S. P. J. *Anal. Chem.* **2007**, *79*, 1153.
(41) Gu, H.; Su, X. D.; Loh, K. P. *J. Phys. Chem. B* **2005**, *109*, 13611.
(42) Davis, F.; Nabok, A. V.; Higson, S. P. J. *Biosens. Bioelectron.* **2004**, *20*, 1531.
(43) Wang, W. U.; Chen, C.; Lin, K.; Fang, Y.; Lieber, C. *Proc. Natl. Acad. Sci. U.S.A.* **2005**, *102*, 3208.

7F2: 5′-GGAGGCTGAGGAAGGAGAAT-3′
7F22: 5′-ATT CTC CTT CCT CAG CCT CC-3′
7R2: 5′-TCCCAAAGCCAGAGAAAAGA-3′
T7: 5′-GCATGAACCG GAGGCCCATC CTCACCAT-CA-3′
T8: 5′-GAACAGCTTT GAGGTGCGTG TTTGTGC-CTG-3′
248G-A: 5′-GCATGAACCG AAGGCCCATC CTCACCAT-CA-3′
P248WT: 5′-GATGGGCCTC CGGTTCATGC-3′

Plasmid pCD-GFP was kindly provided by Prof. Ningshao Xia (School of Life Sciences, Xiamen University). Plasmid PMD18-T was obtained from TaKaRa Biotechnology (Dalian) Co., Ltd. Plasmid DNA was isolated from overnight culture of *Escherichia coli* DH5α using the UNIQ-10 Spin Column Plasmid Mini-Preps Kit from Sangon.

Genomic DNA was isolated from HeLa cells with the UNIQ-10 Spin Column Genomic DNA Isolation Kit from Sangon. Two PCR primers (7F, 7R) were used to amplify a DNA fragment of 108 bp (Rangel-Lopez), a total of 50 μL of PCR reaction mixture containing 10 mM dNTP, 2.5 U Taq DNA polymerase, 250 ng of genomic DNA, 25 mM forward and backward primers, PCR buffer, and 25 mM magnesium chloride. The PCR conditions were as follows: 10 min at 94 °C and then 35 cycles of 15 s at 94 °C for denaturation, 30 s at 55 °C for annealing, and 30 s at 72 °C for elongation, followed by a final extension step of 72 °C for 5 min. PCR product was run on a 2% agarose gel at 150 V for 30 min. The band was cut out of the gel and purified by EZ Spin Column PCR Product Purification Kit from BBI. The concentration of DNA was measured by UV−vis at 260 nm. Samples with OD 260/280 > 1.8 were accepted for further analysis.

Boron-doped diamond film (0.1% or 10^{20} cm^{-3}) on a Si wafer electrode formed when industrial diamond was doped with boron was obtained from Windsor Scientific Limited, U.K. This type of boron-doped diamond was produced in form of free-standing approximately 0.5 mm thick films, which are robust and almost indestructible. Microscopically it is very flat, the specification is 10 nm Ra. The diamond electrode was fixed in an inert Teflon body. The H-terminated BDD electrodes were polished with 0.3 and 0.05 μm alumina slurry on a Buehler polishing cloth and then sonicated in a water bath for 15 min before being used. For the polyethylenimine-coated films, the working electrode was dipped into a 1% solution of polyethylenimine for 5 min, withdrawn, rinsed with water, and allowed to dry. The electrode was next placed in a single-stranded DNA solution (1.6 μg mL^{-1} in water that was denatured by boiling for 5 min) for 5 min and then rinsed.

Alternating current impedance measurements were performed using an electrochemical workstation (CHI660C, CH Instrument) using a 3.0 M KCl−Ag/AgCl as the reference electrode and a platinum (Pt) wire as the auxiliary electrode. Electrodes were immersed in 3 mL of fresh solutions of single-stranded DNA, which were boiled for 5 min and then rapidly cooled to room temperature in ice. The impedance was then measured with time continuously at 10 Hz.

RESULTS AND DISCUSSION

Effect of Frequency on Relative Impedance. Initial experiments were performed with ac impedance measurements across a range of frequencies (1 Hz to 10 kHz) using PEI immobilized ssDNA from PCR fragments of p53 gene, immersed in complementary ssDNA solutions. The plot of relative impedance with frequency failed to show any easily resolvable changes on these scalings, especially at higher frequencies (data not shown). However, when the changes in impedance are plotted with respect to time, differences immediately become apparent. The data for each frequency were therefore processed by dividing the impedance measured at given time intervals by the initial impedance of the BDD electrode immediately following immersion into the DNA solution (Figure 1). It can be seen that a large drop in impedance occurs following exposure to complementary ssDNA, strongly indicating that the change in the AC impedimetric measurements is indeed due to the hybridization of cDNA strands. A similar drop in impedance upon hybridization has been noted by other authors interrogating DNA adsorbed on carbon electrodes and nanotube-modified electrodes.[40,44] Impedance is also seen to decrease with continued cDNA exposure as further hybridization continues. It is possible this behavior can be explained in terms of the higher conductivity of double-stranded DNA (dsDNA) with respect to single-stranded DNA.[45]

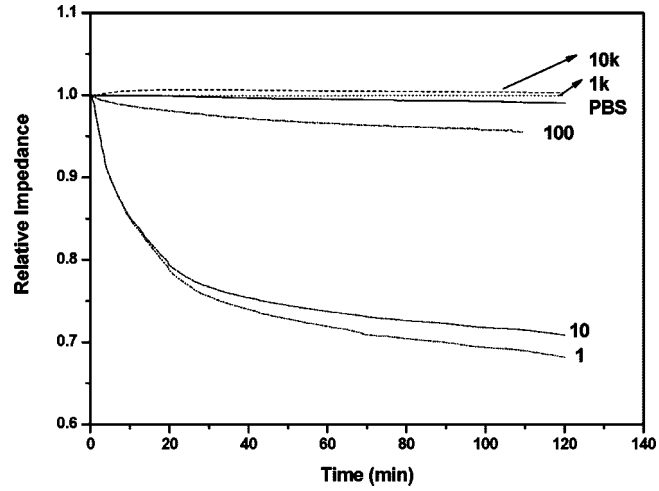

Figure 1. Relative impedance with time at different frequencies for a p53-Exon7 ssDNA-PEI-modified BDD electrode immersed in 1.5 fg mL^{-1} complementary ssDNA/buffer solution as compared to the same electrode immediately following immersion.

It can also be seen that the changes in impedance are more pronounced at lower frequencies upon exposure to cDNA. A large drop in relative impedance was observed at low frequencies of 1 and 10 Hz (Figure 1), and a negligible change was shown at high frequencies of 100 and 1000 Hz and 10 kHz, suggesting that the DNA hybridization primarily leads to a lowering of the capacitance of the interrogated film. The changes observed at lower frequency regions in PEI-modified BDD agree with other polymer-modified electrodes.[40,41] The frequency dependence of this impedance decrease differs from those reported earlier in studies of DNA hybridization using multiwall carbon nanotubes or undoped diamond, where the largest impedance decrease was observed at comparatively higher frequency range.[44] Therefore it is necessary to analyze theoretically the impedance change in different frequency regions. In a general sense, an electrochemical cell can be considered simply an impedance to a small sinusoidal excita-

(44) Cai, H.; Xu, Y.; He, P. G.; Fang, Y. Z. *Electroanalysis* **2003**, *15*, 1864.
(45) Boon, E. M.; Barton, J. K. *Curr. Opin. Struct. Biol.* **2002**, *12*, 320.

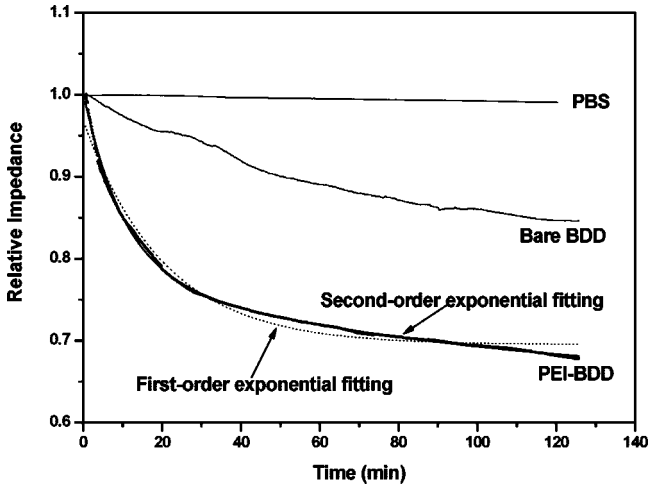

Figure 2. Relative impedance at 10 Hz with time for p53-Exon7 ssDNA-PEI-modified BDD electrode and ssDNA-BDD electrode immersed in 1.5 fg mL^{-1} complementary ssDNA/buffer solution. The dotted lines indicate fits using first- and second-order exponential decays for p53-Exon7 ssDNA-PEI-modified BDD electrode.

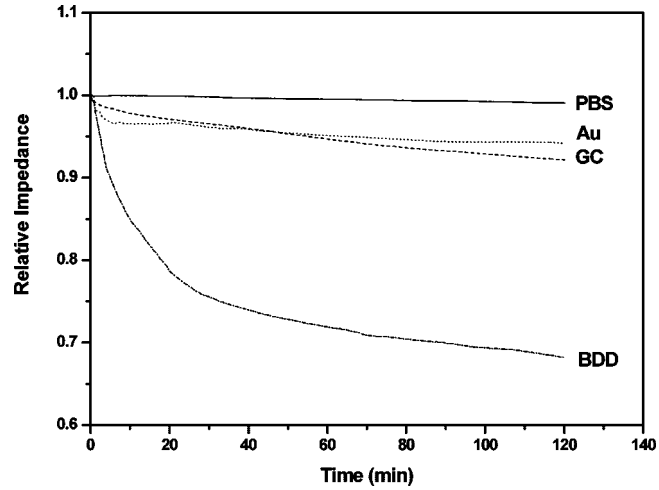

Figure 3. Relative impedance at 10 Hz with time for p53-Exon7 ssDNA-PEI-modified Au, glass carbon (GC), and BDD electrodes immersed in 1.5 fg mL^{-1} complementary ssDNA/buffer solution.

tion; hence, one is able to represent its performance by an equivalent circuit of resistors and capacitors that pass current with the same amplitude and phase angle that the real cell does under a given excitation.[46] The frequency dependence in low-frequency regime comes only from Warburg impedance terms; thus, the linear correlation of Z_{Re} and Z_{Im} is characteristic of a diffusion-controlled electrode process. As the frequency rises, the charge-transfer resistance, R_{ct}, and the double-layer capacitance become more important elements. At very high frequencies, the Warburg impedance becomes unimportant in relation to R_{ct}. The imaginary component to the impedance comes solely from C_d. Its contribution falls to zero at high frequencies, because it offers no impedance. All of the current is charging current, and the only impedance it sees is the ohmic resistance.[46] In our system, the ac impedance was measured at a potential of 5 mV. Under this condition, there is no oxidation−reduction chemistry taking place and the measurements are a very gentle way of measuring the intrinsic electrical properties of the interface. The charge-transfer process is negligible, and the diffusion-controlled process is an important one; the Warburg impedance becomes important. Therefore the following ac impedance measurements were at a fixed low frequency (10 Hz) because the signal-to-noise ratio was low at the frequency of 1 Hz.

Effect of PEI on Relative Impedance. A large drop in relative impedance was observed at the PEI-modified BDD electrode in comparison to the bare BDD electrode (Figure 2). From this result, it appears that DNA hybridization at a positively charged polymer surface leads to an overall drop in impedance. This observation is similar to that reported previously for the PEI-modified carbon electrode for single gene differentiation.[40] The thickness of the PEI layer is about 5.0 nm and decreases the capacitance which was confirmed by the $Fe(CN)_6^{4-/3-}$ system voltammetric responses. Many researchers have studied the immobilization of DNA on electrodes surfaces by a wide variety of methods.[47] Some researchers have used electrostatic interaction between DNA and cationic surfaces, for example, by modifying a surface with a polymeric amine. Other researchers have used electrodeposition onto screen-printed carbon, pretreatment of glass slides with PEI solution, or deposition onto amino-silanized glass to immobilize DNA on the electrode surface. Other work demonstrated that LB films of octadecylamine deposited from subphases containing *E. coli* plasmid DNA incorporated the DNA in a single-stranded form between the layers. Soaking these systems in solutions of single-stranded DNA was found to lead to further incorporation of DNA. Hybridization of cDNA was shown to occur selectively, although whether actual formation of a DNA double helix occurs is still in doubt, and it is possible that a nonhelical duplex may be the preferred structure.[48] The improvement of sensitivity by a positively charged PEI layer will be further discussed in the final section.

Effect of Electrode on Relative Impedance. The principal motivation for investigating diamond thin films is the possible use of molecularly modified diamond thin films as chemical or biological sensing elements. Because gold (Au) and glass carbon (GC) electrodes remain the most widely used electrode materials, a comparison of functionalized diamond and functionalized Au and GC surfaces is warranted. Figure 3 plots the relative impedance for PEI/p53 gene ssDNA-PEI-modified Au, GC, and BDD electrodes immersed in 1.5 fg mL^{-1} complementary ssDNA/buffer solution. A large drop in relative impedance was observed at PEI-modified BDD electrode in comparison to PEI-modified Au and GC electrodes. This result is attributed to a relatively low background current and very low double-layer capacitance of BDD electrodes in comparison to Au and GC electrodes. Work of our group and others has shown that diamond can be used as an electrode material with higher sensitivity than Au and GC electrodes in electroanalysis.[4−10] Some research has shown that diamond thin films exhibit many of the properties expected for a p-type semiconductor. In particular, the field effect, in which an external potential induces an electric field that penetrates into the subsurface region of the diamond, alters its conductivity. Diamond

(46) Bard, A. J.; Faulkner, L. R. *Electrochemical Methods: Fundamentals and Applications*, 2nd ed.; John Wiley and Sons: New York, 2000; pp 376–386.

(47) Gooding, J. *Electroanalysis* **2002**, *14*, 1149.

(48) Lemeshko, S. V.; Powdrill, T.; Belosludtsev, Y. Y.; Hogan, M. *Nucleic Acids Res.* **2001**, *29*, 3051.

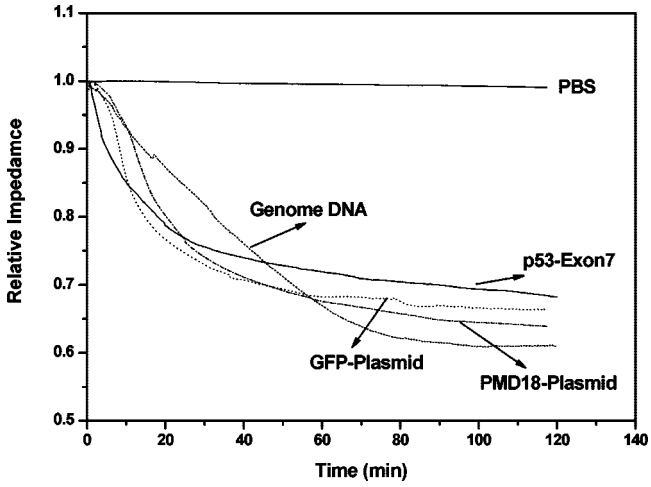

Figure 4. Relative impedance at 10 Hz with time for the p53-Exon7 ssDNA-PEI-modified BDD electrode immersed in 1.5 fg mL^{-1} complementary ssDNA/buffer, GFP-plasmid, PMD18-plasmid DNA, and genome DNA/buffer solutions, respectively.

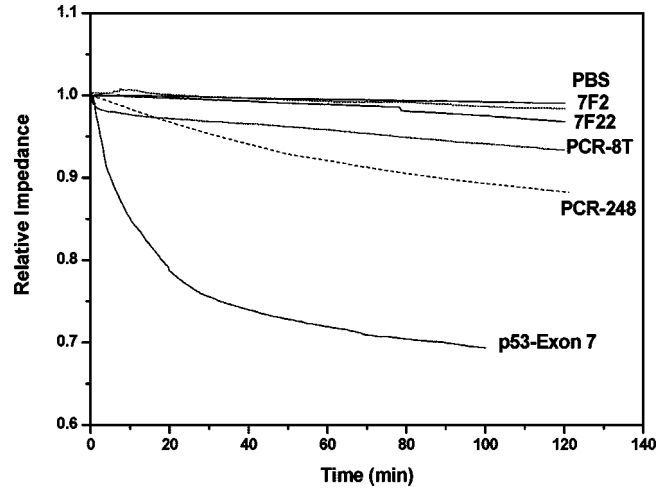

Figure 5. Relative impedance at 10 Hz with time for the p53-Exon 7 ssDNA-PEI-modified BDD electrode immersed in 1.5 fg mL^{-1} complementary ssDNA/buffer and 1.0 ng mL^{-1} noncomplementary ssDNA/buffer solutions.

surfaces are relatively free of charge-trapping defects, and over a substantial part of the frequency range the impedance is dominated by the diamond space-charge layer, exhibiting a significant "field effect" in response to an external potential.[49] The improvement of sensitivity by a BDD electrode will be further discussed in the final section.

Effect of Plasmid DNA on Relative Impedance. The introduction of cDNA was found to give rise to changes in impedance that could be measured. The presence of the plasmid DNA would prevent the electrode from being sequence-selective.[40] Alternating current impedance data of single-stranded PCR-DNA/PEI immobilized films upon plasmid DNA exposure were therefore determined for comparison. Figure 4 shows impedimetric changes following exposure to 1.5 fg mL^{-1} complementary PCR fragments of p53 gene and noncomplementary GFP-plasmid and PMD18-plasmid DNA. As can be seen, very similar results are obtained in all three cases. However, the binding kinetics were different for the curves in Figure 4. Initially the complementary ss-DNA in solution was quickly adsorbed and hybridized with the complementary ss-DNA on PEI-modified BDD electrode surface before 10 min, and a larger impedance drop for the complementary ss-DNA was observed than plasmid DNA. Then after 25 min, a larger impedance drop for plasmid DNA was observed than for the complementary ss-DNA, which suggests more plasmid DNAs were adsorbed into the positively charged PEI-modified BDD electrode surface than the complementary ss-DNA at final stage. To the best of our knowledge, a low-molecular weight polymer would have quicker adsorbing kinetics than a high-molecular weight one at the first stage, but the high-molecular weight polymer absorbs more amounts on the surface than the low-molecular weight one at the last stage. The result was also observed in PEI-modified carbon electrode for single gene differentiation.[40] Therefore all ac impedance measurements utilized PCR-DNA without plasmid DNA to improve the selectivity of BDD electrode.

Effect of Genome DNA on Relative Impedance. The genome DNA has the same fragments with PCR products from Exon 7 of the human p53 gene. Therefore it is necessary to discuss the effect of genome DNA on impedimetric changes. Figure 4 also shows impedimetric changes following exposure to genome DNA. The curve shape and binding kinetics are similar to plasmid DNA shown in Figure 4. While the genome DNA has a much higher molecular weight than PCR-DNA at first stage (before 45 min), the low-molecular weight complementary ss-DNA was quickly adsorbed and hybridized with the complementary ss-DNA on the electrode surface, and a larger impedance drop was observed (Figure 4). The genome DNA also has the same complementary fragments with PCR ss-DNA and would hybridize with complementary ss-DNA on the electrode surface. However the genome DNA has a long chain which would prevent the electrode from being sequence-selective at the initial stage. With time increasing, the genome DNA chain would change morphology to expose complementary fragments and hybridize with complementary ss-DNA on the electrode surface at the last stage and a larger impedance drop for genome DNA was observed.

Effect of Noncomplementary ssDNA on Relative Impedance. From the above results, the introduction of cDNA was found to give rise to changes in impedance that could be measured and the presence of the plasmid and genome DNA would prevent the electrode from being sequence-selective. Alternating current impedance data of single-stranded p53-Exon 7/PEI-immobilized films upon noncDNA exposure were therefore determined for comparison. Further experiments were then made by exposing samples to varying concentrations of noncDNA. Results shown (Figure 5) are for a PEI/p53-Exon 7 ssDNA-PEI-modified BDD electrode exposed to two PCR-DNAs and two DNA oligonucleotides. As can be seen at the 1.5 fg mL^{-1} level, there is good selectivity with a large change in impedance for the cDNA solution but minimal changes for noncomplementary even if higher concentrations (1.0 ng mL^{-1}) of ssDNA were used. There are negligible impedance changes when lower concentrations of noncDNA are used (for clarity, data not shown). In some cases, lower concentrations of noncDNA lead to an increase in impedance. One possible explanation is that within polyelectrolyte self-assembled layers, solvated polymers can sometimes displace the

(49) Tse, Y.; Nichols, B. M.; Yang, W.; Butler, J. E., Jr.; Hamers, R. J. *J. Phys. Chem. B* **2005**, *109*, 8523.

polymers bound to the surface,[50] and a second possibility is an oligonucleotide can be desorbed from positively charged surfaces.[51]

Effect of Nonspecific Binding on Relative Impedance. Negatively charged bovine serum albumin (BSA) was used to block nonspecific interactions. Initially, BDD electrodes coated with PEI and ssDNA were constructed and soaked for 1 h in a 1% solution of BSA. However, the resultant electrodes displayed a slow decrease in impedance when immersed in PBS buffer alone. Addition of 1.5 fg mL^{-1} complementary ssDNA had no additional detectable effect, suggesting that BSA could be slowly desorbing from the electrode surface. This effect approached a plateau after about 4 h, and again the resultant films displayed almost no change in impedance when exposed to cDNA. Either there is an adsorbed layer of BSA remaining that blocks access of the DNA probe or there has been a complete displacement of DNA from the surface of the electrode by the negatively charged BSA.

Electrochemical Detection Using PCR DNA. These above results show the sensitivity of the technique; however, the presence of the plasmid DNA, genome DNA, and negatively charged protein prevented the BDD electrode from being sequence-selective. We modified the investigations in four ways: (1) increasing the sensitivity by continuously monitoring the impedance at 10 Hz, rather than scanning across a range of frequencies, (2) improving selectivity by utilizing short DNA strands produced by PCR and without plasmid, (3) increasing the sensitivity by utilizing PEI-coated BDD electrodes instead of bare BDD, and (4) removing a majority of proteins to obtain purified DNA strands produced by PCR and further purified by EZ Spin Column. The electrochemical system is not well defined by means of ultrastructure analysis; however, the electrochemical data can provide the kinetic parameters of DNA adsorption and hybridization. The following section will discuss the kinetic process of DNA adsorption and hybridization.

To compare our results with those obtained previously,[40,42,44] the mean change in impedance over the frequency spectra were recorded for a variety of concentrations and plotted against time in Figure 6. All of the electrodes showed a drop in mean impedance against time; however, this was dependent on the concentration of cDNA in solution. It can be seen in Figure 6 that concentration of 10^{-19} g mL^{-1} of ssDNA can be detected using this method. Increasing the concentration of ssDNA led to faster hybridization; however, the relationship between impedance and concentration was not simply linear. Figure 6b shows the calibration plot of relative impedance and logarithmic concentration, which is linear ($Z = -0.104 - 0.053 \log C$, correlation coefficient of 0.988) with the ssDNA concentration from 10^{-20} to 1.0 pg mL^{-1}. The maximum sensitivity seemed to occur at a concentration of 1 pg mL^{-1}, with further increase in concentration actually appearing to reduce the sensitivity, indicating that the sensor became saturated. The sensitivity obtained was greater than those found in refs 40, 42, and 44.

Higher concentrations lead to an initial higher rate of adsorption and hybridization, probably due to a simple diffusional gradient, and it should also be noted that the plots of impedance versus time tend toward plateaus at shorter times, indicating saturation had occurred. As discussed in Effect of Frequency on Relative Impedance, the ac impedance measurements were at a fixed frequency (10 Hz), the diffusion-controlled process is an important one in our system, and the Warburg impedance becomes important. Increasing the concentration from 1.0 fg mL^{-1} to 1.0 μg mL^{-1} has a minimal effect on the initial rate of hybridization (for simplicity, data of higher concentrations not shown), suggesting that a different process has become the rate-limiting step.[40] We can therefore conclude the DNA concentration imparts diffusional control of DNA mass transport to the BDD electrode surface, although above certain concentrations, the rate of DNA hybridization acts as a rate-limiting step. The BDD electrode response to DNA hybridization is therefore under mixed mass transport and kinetic control.

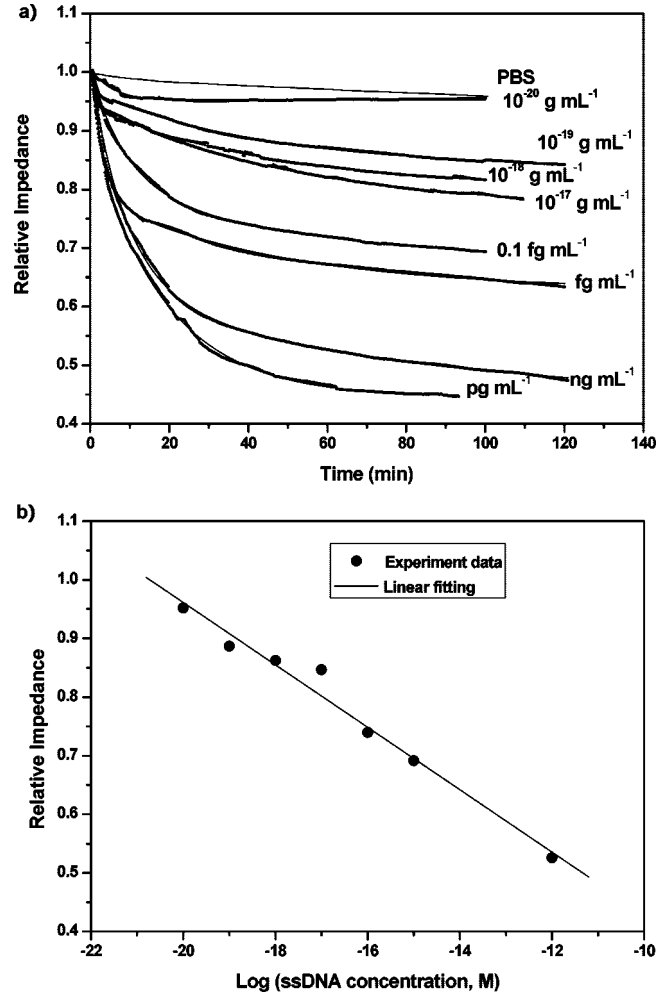

Figure 6. (a) Relative impedance at 10 Hz with time for p53-Exon7 ssDNA- PEI-modified BDD electrodes scanned while being immersed in various concentrations of complementary ssDNA/buffer solution. The solid lines indicate fits using second-order exponential decays. (b) Calibration plot of relative impedance at 40 min for determination ssDNA at p53-Exon7 ssDNA-PEI-modified BDD electrodes.

Fitting of Experimental Data. The curve reveals a decay against time and could be fitted to a first-order (eq 1) or second-order (eq 2) exponential decay as indicated by the dotted lines (Figure 2). The fitting of second-order exponential decay could overlap with our experimental data and is better than that of first-

(50) Lavalle, P.; Vivet, V.; Jessel, N.; Decher, G.; Voegel, J. C.; Mesini, P. J.; Schaaf, P. *Macromolecules* **2004**, *37*, 1159.
(51) Chan, V.; Graves, D. J.; Fortine, P.; Mckenzie, S. E. *Langmuir* **1997**, *13*, 320.

order experimental fitting. This result is reasonable because the PEI-modified BDD electrode response to DNA hybridization has adsorption and hybridization steps and is under mixed mass transport and kinetic control. Therefore, the second-order exponential decay was used to fit all impedance measurements of various concentrations. The calculated rate constants for both steps were 9.81×10^{-2} s^{-1} for ssDNA adsorption and 9.78×10^{-3} s^{-1} for ssDNA hybridization. The calculated rate constants for the adsorption and hybridization of ssDNA onto the PEI-modified BDD electrode agree reasonably well with the reported rate constants of DNA adsorption and hybridization onto PEI-modified SiO_2, which have the calculated values of 5.52×10^{-2} s^{-1} for DNA adsorption and 2.41×10^{-3} s^{-1} for DNA hybridization.[52]

$$Z(t) = Z_0 + \Delta Z \exp(-t/\tau) \quad (1)$$

$$Z(t) = Z_0 + \Delta Z_1 \exp(-t/\tau_1) + \Delta Z_2 \exp(-t/\tau_2) \quad (2)$$

Fitting the impedance data to eq 2 yields the characteristic adsorption times τ_{adsorb} from 10 to 1 min with increasing DNA concentration from 10^{-19} g mL^{-1} to 1 ng mL^{-1} and the hybridization times τ_{hybrid} from 50 to 20 min with increasing DNA concentration from 10^{-19} g mL^{-1} to 1 ng mL^{-1}, reaching a final plateau approximately 40 min after electrode immersion. The result is similar to the reported time of ssDNA hybridization on DNA-covalently modified diamond.[53,54] At 40 min, a measurement can be registered to obtain quantitative measurement of DNA. This time is shorter than those of the classical methods with radioactive and optical labeling (hours to days). In order to further decrease the measurement time, the dimension of the electrochemical cell was decreased from 3 mL to 100 μL. However, the measurement time is not obviously decreased. The result is similar to the reported time of ssDNA hybridization on DNA-covalently modified diamond which the dimension of the electrochemical cell is 100−200 μL.[54] The result is reasonable because the rate constant of hybridization of DNA (9.78×10^{-3} s^{-1}) is lower than the rate constant of adsorption of DNA (9.81×10^{-2} s^{-1}). On the other hand, the measurement temperature would affect the adsorption and hybridization of DNA. The T_m of the p53-Exon 7 is 55 °C, usually the optimal hybridization temperature is about 30 °C (T_m − 25 °C). Therefore, the measurement temperature was increased from 25 to 40 °C. The measurement time was decreased from 40 to 30 min and decreasing time is not very obvious because the measurement time is determined by the DNA hybridization rate constant.

Reproducibility. We have attempted to reverse the hybridization. Heating the BDD electrodes or electrostatic polarization may reverse hybridization and regenerate the sensor. However, this process did not work well when the solution was heated because we simply did not remove all of the DNAs from the electrodes or some PEI would desorb from the BDD electrode. The BDD electrode could be regenerated when 0.05 M NaOH was used to denature the dsDNA. The reproducibility of the immobilized DNA probe was further confirmed by denaturing the DNA duplex using 0.05 M NaOH and then followed by rehybridization with cDNA. Figure 7 shows the relative impedance at 10 Hz at 40 min for a p53 gene-Exon 7 ssDNA-PEI-modified BDD electrode immersed in 1.5 fg mL^{-1} complementary ssDNA/buffer after repeated hybridization and denaturation. The constant value of relative impedance before seven cycles proves that PEI-modified BDD electrode is stable. The relative impedance increased after seven cycles, which means the low adsorption and hybridization of DNA leads to the impedance increases. The low adsorption and hybridization of DNA may result from desorption of PEI from BDD electrode after repeated denatureing in 0.05 M NaOH. Another alternative was to remove and clean PEI and DNA from the BDD electrode surface by polishing with a 0.3 and 0.05 μm alumina slurry on a Buehler polishing cloth, then sonicating in a water bath for 15 min, and then recoating PEI and ssDNA on the electrode again; after such treatment, the stability and reproducibility of the BDD electrode is good. We also used this method to regenerate the Au cluster-modified BDD electrode.[10] However, for this to be feasible, there must be good reproducibility both from run-to-run and also from electrode-to-electrode. We found repeated runs on the same electrode were reproducible with RSDs < 4%. We have also determined the electrode-to-electrode reproducibility of sensor response to have RSDs < 9% variability in a series of trials. This RSD value is a little high because we cannot fabricate the BDD electrodes with the same area with simple treatment of homemade BDD. Therefore it is necessary to investigate the effect of the electrode area on relative impedance. We fabricated four electrodes with areas of 0.014, 0.034, 0.11, and 0.14 cm^2. A large drop in relative impedance would occur for four electrodes when cDNA was used. Good sensitivity was also observed for levels down to 10^{-18} g mL^{-1} for 0.014 and 0.034 cm^2 electrodes and 10^{-19} g mL^{-1} for 0.11 and 0.14 cm^2 electrodes. All impedance measurements used 0.11 cm^2 electrodes in this research unless stated otherwise. As discussed above, the diffusion-controlled process is an important one, the smaller electrode area imparts diffusion control of DNA mass transport to the BDD electrode surface.

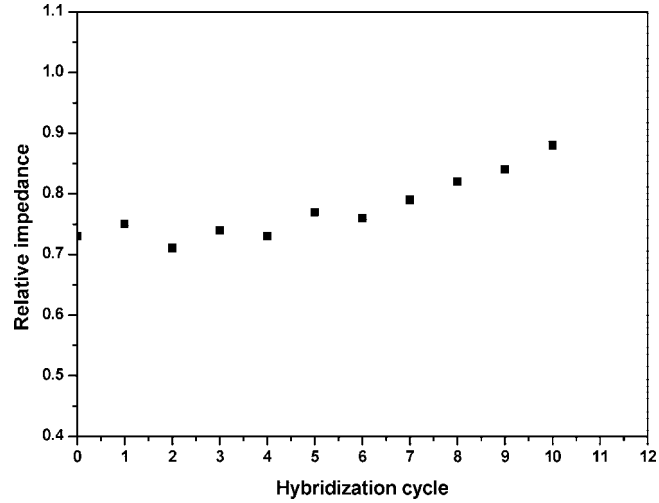

Figure 7. Relative impedance at 10 Hz at 40 min for a p53 gene-Exon 7 ssDNA-PEI-modified BDD electrode immersed in 1.5 fg mL^{-1} complementary ssDNA/buffer after repeated hybridization and denaturation.

(52) Rawle, R. J.; Selassie, C. R. D.; Johal, M. S. *Langmuir* **2007**, *23*, 9563.
(53) Yang, W.; Butler, J. E.; Russell, J. N.; Hamers, R. J. *Langmuir* **2004**, *20*, 6778.
(54) Vermeeren, V.; Bijnens, N.; Wenmackers, S.; Daenen, M.; Haenen, K.; Williams, O. A.; Ameloot, M.; vandeVen, M.; Wagner, P.; Michiels, L. *Langmuir* **2007**, *23*, 13193.

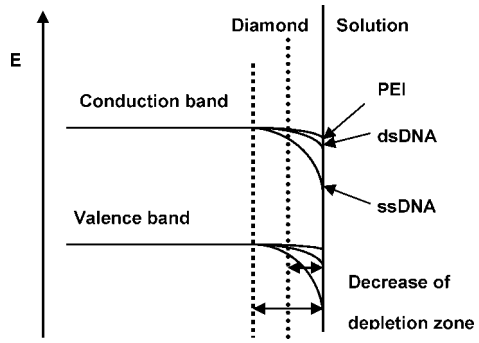

Figure 8. Schematic representation of the energy diagram at the PEI-coated diamond−solution interface. Extra negative charges, located at the surface during hybridization, will decrease the electric field and reduce the band bending in the space charge region.

Field Effect and Surface Charge Density. Our data show that the hybridization-induced changes in impedance observed at low frequencies arise primarily from a field effect in which the negative charge of DNA molecules hybridizing with their surface-bound complements induces an upward band-bending in the diamond space-charge region (Figure 8). The similar figure has previously been proposed by Yang[53] and Vermeeren[54] to explain the hybridization-induced changes in electrical properties of DNA-modified diamond surfaces. The decreasing impedance and increasing conductivity of diamond can be rationalized in terms of the depletion zone in the space charge region of a semiconductor during DNA hybridization. This depletion zone is a result of the exchange of charges at a semiconductor−solution interface. For a p-type semiconductor, when equilibrium is reached, the resulting electric field at the interface corresponds to a downward band bending of the conduction and the valence band.[55] A decrease of the depletion zone is explained in Figure 8. When transferring from ssDNA to dsDNA, negatively charged DNA strands are adsorbed at diamond surface, and as a result the depletion zone will become smaller. Only in the lowest frequency region from 1 to 100 Hz, the $R_{ct}C$ element influences the impedance. The $R_{ct}C$ element has been attributed to the layer of molecules and ions at the surface. It has also been reported in the literature that ssDNA is less conductive than dsDNA.[45] Both factors can explain a decrease of the impedance in the double-layer region after hybridization.

The size of this field effect (and the resulting change in impedance of the diamond) is controlled by a number of different factors. Previous studies of semiconductor−electrolyte interfaces have shown that the capacitance associated with the ions in solution (the double-layer) is typically much larger than the capacitance associated with the semiconductor space charge region.[56,57] This field effect of p-type semiconductor diamond is observed in our system when compared with conductors Au and GC electrodes (Figure 3). Consequently, specific adsorption of ions at the interface leads to significant changes in potential within the semiconductor but only small changes in potential within the electrolyte solution. Using the depletion approximation, the surface charge density is given by

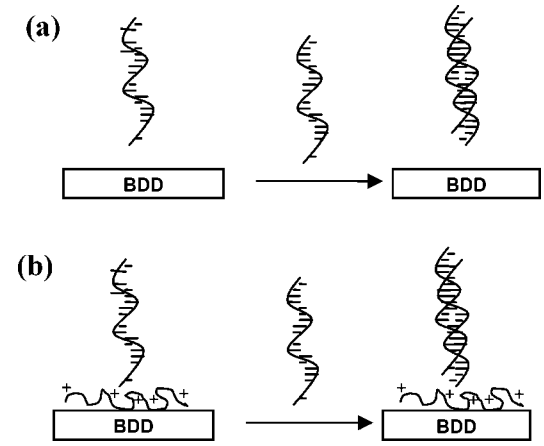

Figure 9. Schematic representation of surface charge distribution before and after DNA hybridization: (a) without PEI at the surface of BDD and (b) PEI-coated BDD.

$$\sigma_{surface} = \sqrt{\frac{2k\varepsilon_0 N_A V}{q}} \quad (3)$$

where $\sigma_{surface}$ is the number of charges per unit area, N_A is the concentration of acceptors, and V is the change in potential between the surface and bulk, also referred to as the "band-bending". The equation has previously been proposed by Yang[53] to calculate the surface charge density of diamond. Subtracting the surface charge density before and after hybridization (using $V = 1.67$ and 1.47)[53] leads to the conclusion that the charge density within the semiconductor bulk changes by $\sim 3 \times 10^{11}$ electrons/cm^2 upon DNA hybridization. It has reported previously[37,53] that the number density of DNA molecules hybridized to the diamond surface is approximately 3×10^{12} molecules/cm^2, with each DNA molecule carrying multiple negative charges.

The above analysis shows that the total change in charge within the space-charge layer is significantly smaller than the charge associated with the hybridizing DNA molecules. We believe this has three possible origins. First, we note that the negative charge on the DNA backbone is partially compensated for by PEI or loosely bound cations. A second contributing factor is that surface states at the semiconductor−electrolyte interface (such as unterminated surface "dangling bonds") can screen the diamond from the negative charge of the hybridizing DNA molecules, thereby reducing the field effect. Finally, because the DNA molecules are separated from the diamond surface by positive charged PEI, it is likely that DNA hybridization induces significant charge redistribution within the double-layer of DNA and PEI (Figure 9). Our experimental data also support this result that PEI would induce significant charge redistribution within the surface of BDD. The decreasing of impedance was lower at the bare BDD electrode without PEI than that of the PEI-coated BDD electrode after DNA hybridization (Figure 2). The experimental result proved that DNA hybridization would induce significant charge redistribution within the double-layer of DNA and PEI.

CONCLUSIONS

We have described the PEI-modified BDD electrodes incorporating single-stranded DNA for detection of DNA hybridization. These

(55) Memming, R. In *Semiconductor Electrochemistry*; Wiley-VCH: Weinheim, Germany, 2000.
(56) Rajeshwar, K. In *Semiconductor Electrodes and Photoelectrochemistry*; Licht, S., Bard, A., Eds.; Wiley-VCH: Weinheim, Germany, 2002; Vol. 6.
(57) Singh, P.; Singh, R.; Gate, R.; Rajeshwar, K.; DuBow, J. *J. Appl. Phys.* **1980**, *51*, 6286.

hybridization events have been interrogated by an ac impedimetric approach at a fixed frequency (10 Hz) with the results showing that cDNA hybridization gives rise to a lowering of the capacitive properties of the BDD electrode/PEI film in solution. Good sensitivity was also observed for levels down to 10^{-19} g mL^{-1}. The hybridization process was shown to be sequence specific in that noncomplementary single-stranded DNA had no comparable electrical effect. The present electrical measurements likewise show that the modified films have a low surface state density that permits the charged biomolecules to induce a significant field effect and charge redistribution. Even though the method requires a highly purified sample in order to achieve selectivity and PCR amplification of the target DNA in order to achieve sensitivity, this high degree of sample pretreatment is a major disadvantage if this method is to be considered a DNA probe. The PEI-modified BDD electrode developed is a novel sensor with high sensitivity and inexpensive to manufacture and offers many advantages in comparison to those that require labels.

ACKNOWLEDGMENT

This work is supported by 973 Program No. 2006CB933300, Program for New Century Excellent Talents in Fujian Province (Grant No. Z03131), Natural Science Foundation of China (Grant No. 20701031), Natural Science Foundation of Fujian Province of China (Grant No. C0710045), Open Fund of State Key Laboratory for Physical Chemistry of Solid Surfaces, Xiamen University (Grant No. 200602), and Science and Technology Innovation Project of Fujian Province for Young Scientific Researchers, China (Grant No. 2006F3128).

Received for review March 26, 2008. Accepted July 18, 2008.

AC800610Z